Chemical Engineering Journal 86 (2002) 53–60

Chemical Engineering Journal

www.elsevier.com/locate/cej

Model based predictive control of a rotary dryer

Helge Didriksen

dk-Teknik, Energy & Environment, Gladsaxe Møllevej 15, 2860 Søborg, Denmark

Abstract

A dynamic model describing the transfer of mass, energy and momentum has been developed for a rotary dryer. The model is applied to an industrial case, drying of sugar beet shreds at a Danish sugar factory. The model is fitted to plant data and shows a good ability in predicting variations in product quality with changes in manipulated variables and disturbances. A comparison is made, in a simulation study, with traditional feedback control and model based predictive control (MPC) with feedforward action.

Keywords: Rotary dryer; First principles modeling; Model based predictive control; Augmented Kalman filter; Sugar beet drying

1. Introduction

Sugar is extracted from sugar beets in direct contact with water in "diffusers". The beets have been cut into thin strips, to ensure effective extraction. From the diffusers, wet beet pulp is carried through pulp presses. The juice from the presses contains some sugar and is returned to the diffusers. The pressed beet pulp still contains approximately 70–75% moisture. The purpose of the dryer is to reduce the moisture content down to approximately 10%. The dried sugar beet pulp can be utilized as animal feed.

2. The rotary dryer process

The sugar beet pulp dryer is a horizontal rotating drum. The inside of the dryer is fitted with lifters to promote intimate contact between the wet solid and the hot gases. The drum is a co-current dryer. The pulp is transported along the length of the dryer mainly as a result of the drag from the hot gas flow on the solids falling from the lifters. The water content in the pulp evaporates as the pulp progresses along the dryer. The energy input to the dryer is provided by a coal fired gas generator. Secondary air into the gas generator is mainly recirculated exhaust air from the dryer.

3. Model of a rotary dryer

The model presented here is a first principle model based upon conservation of mass, energy, and momentum. The model describes the longitudinal motion of the mass of gas and solid, the heat transfer from gas to solid, the mass transfer from solid to gas and the intra-particle effects; water diffusion and heat conduction. The model is based upon various sources, the most important are Marinos-Kouris and Maroulis [1], Courtois [2] and Perry and Green [3].

3.1. Conceptual model

There are very large gradients in most process variables in the rotary dryer, especially in gas temperature and also in moisture contents in both gas and solid phase. It is necessary to treat the process as a distributed parameter system. To deal with this, the model is fundamentally represented as a number of CSTR in series. The process is divided into imaginary volume elements. Mass and energy is exchanged between the elements as shown in Fig. 1. In this work, $N = 10$ volume elements is used. Following assumptions are made:

- Heat and mass transfer from the drying gas to the solid particles takes place when the particles fall from the internal dryer flights into the drying gas stream (Fig. 2).
- There are no gradients in temperatures and moisture contents in each volume element.
- The thermal properties of solid and gas are functions of temperatures and moisture contents.
- The area available for mass and energy transfer between gas and solid equals the sum of the particle area of the suspended mass.

To account for water diffusion and heat conductance resistances in the particle, the particle is divided into three layers. Heat and mass is transferred from one layer to the next as shown in Fig. 3. Heat is transferred from the gas to the outer layer of the particle by convection and radiation. Water is evaporated from the outer layer of the particle.

E-mail address: hdidriksen@dk.teknik.dk (H. Didriksen).

1385-8947/02/$ – see front matter
PII: S1385-8947(01)00272-8

Nomenclature

a	acceleration (m/s^2)
A	area (m^2/s)
c_p	specific heat capacity (constant pressure) (kJ/kg °C)
C_D	drag force coefficient (–)
C_v	total heat capacity (constant volume) (kJ/°C)
d	particle diameter (m)
D	dryer inner diameter *or* solid diffusivity (m, m^2/s)
D'	diffusion coefficient (kg/sm^2)
F_D	drag force (N)
g	gravity acceleration (m/s^2)
h	heat transfer coefficient (kW/Cm^2)
j	molar flux or heat/mass transfer factor (mol/s)
k	mass transfer coefficient (kg/sm^2)
L_eff	dryer inner (effective) length (m)
m	mass (kg)
M	molar weight *or* percentage of moisture (kg/mol, 100 × kg/kg)
n	number of moles (–)
N	number of volume elements *or* drum rot. speed (–, rev/s)
p	partial pressure (kPa)
P	pressure (kPa)
Q	heat transfer (kJ/s)
s	distance (m)
t	time (s)
T	temperature (°C)
U	energy (kJ)
v	linear velocity (m/s)
w	mass flow (kg/s)
X	moisture (kg/kg)
Y_av	average height of fall of particle in a cascade (m)

Greek letters

α	drum slope angular (°)
ε	emmitance
λ	thermal conductivity (kW/m °C)
μ	dynamic viscosity (kg/ms)
θ	tuning parameters
ρ	density (kg/m^3)
σ	Boltzman's constant

Subscripts

cond	conduction
conv	convection
d	dry content
diff	diffusion
evap	evaporation
g	gas
i	volume element number
rad	radiation
s	solid
w	water/moisture

A number of state variables describe the condition in each volume element. The state variables in each volume element are in Table 1.

The total number of moles in the gas phase is also a state variable. (Note that the mass of dry air/combustion gas are not state variables.)

A number of ordinary differential equations are obtained by deriving the mass and energy balances for the solid phase and gas phase of each volume element.

3.2. Conservation of mass

$$\frac{\mathrm{d}m_{\mathrm{sw},1,i}}{\mathrm{d}t} = w_{\mathrm{sw},1,i-1} - w_{\mathrm{sw},1,i} - w_{\mathrm{evap},i} + w_{\mathrm{diff},21,i} \quad (1)$$

$$\frac{\mathrm{d}m_{\mathrm{sw},2,i}}{\mathrm{d}t} = w_{\mathrm{sw},2,i-1} - w_{\mathrm{sw},2,i} - w_{\mathrm{diff},21,i} + w_{\mathrm{diff},32,i} \quad (2)$$

$$\frac{\mathrm{d}m_{\mathrm{sw},3,i}}{\mathrm{d}t} = w_{\mathrm{sw},3,i-1} - w_{\mathrm{sw},3,i} - w_{\mathrm{diff},32,i} \quad (3)$$

$$\frac{\mathrm{d}m_{\mathrm{sd},i}}{\mathrm{d}t} = w_{\mathrm{sd},i-1} - w_{\mathrm{sd},i} \quad (4)$$

$$\frac{\mathrm{d}m_{\mathrm{gw},i}}{\mathrm{d}t} = w_{\mathrm{gw},i-1} - w_{\mathrm{gw},i} + w_{\mathrm{evap},i} \quad (5)$$

3.3. Conservation of energy

$$\frac{\mathrm{d}U_{\mathrm{g},i}}{\mathrm{d}t} = (w_{\mathrm{gc},i-1}c_{p,\mathrm{gc}} + w_{\mathrm{gw},i-1}c_{p,\mathrm{gw}})T_{\mathrm{g},i-1} - (w_{\mathrm{gc},i}c_{p,\mathrm{gc}} + w_{\mathrm{gw},i}c_{p,\mathrm{gw}})T_{\mathrm{g},i} + w_{\mathrm{evap},i}c_{p,\mathrm{gw}}T_{\mathrm{g},i} - Q_{\mathrm{conv},i} - Q_{\mathrm{rad},i} \quad (6)$$

$$\frac{\mathrm{d}U_{\mathrm{s},1,i}}{\mathrm{d}t} = (w_{\mathrm{sd},1,i-1}c_{p,\mathrm{d}} + w_{\mathrm{sw},1,i-1}c_{p,\mathrm{w}})T_{\mathrm{s},1,i-1} - (w_{\mathrm{sd},1,i}c_{p,\mathrm{d}} + w_{\mathrm{sw},1,i}c_{p,\mathrm{w}})T_{\mathrm{s},1,i} + w_{\mathrm{diff},21,i}c_{p,\mathrm{w}}T_{\mathrm{s},2,i} - w_{\mathrm{evap},i}h_{\mathrm{evap}} + Q_{\mathrm{conv},i} + Q_{\mathrm{rad},i} - Q_{\mathrm{cond12},i} \quad (7)$$

$$\frac{\mathrm{d}U_{\mathrm{s},2,i}}{\mathrm{d}t} = (w_{\mathrm{sd},2,i-1}c_{p,\mathrm{d}} + w_{\mathrm{sw},2,i-1}c_{p,\mathrm{w}})T_{\mathrm{s},2,i-1} - (w_{\mathrm{sd},2,i}c_{p,\mathrm{d}} + w_{\mathrm{sw},2,i}c_{p,\mathrm{w}})T_{\mathrm{s},2,i} - w_{\mathrm{diff},21,i}c_{p,\mathrm{w}}T_{\mathrm{s},2,i} + w_{\mathrm{diff},32,i}c_{p,\mathrm{w}}T_{\mathrm{s},3,i} + Q_{\mathrm{cond12},i} - Q_{\mathrm{cond23},i} \quad (8)$$

$$\frac{\mathrm{d}U_{\mathrm{s},3,i}}{\mathrm{d}t} = (w_{\mathrm{sd},3,i-1}c_{p,\mathrm{d}} + w_{\mathrm{sw},3,i-1}c_{p,\mathrm{w}})T_{\mathrm{s},3,i-1} - (w_{\mathrm{sd},3,i}c_{p,\mathrm{d}} + w_{\mathrm{sw},3,i}c_{p,\mathrm{w}})T_{\mathrm{s},3,i} - w_{\mathrm{diff},32,i}c_{p,\mathrm{w}}T_{\mathrm{s},3,i} + Q \quad (9)$$

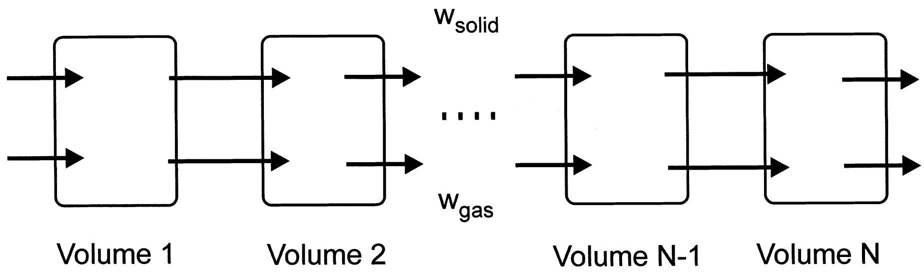

Fig. 1. CSTR's in series.

A temperature explicit form of the energy balances can be derived from:

$$\frac{d}{dt}U = \frac{d}{dt}(C_v T) = \frac{dC_v}{dt}T + \frac{dT}{dt}C_v \tag{10}$$

where C_v denotes the heat capacity of the total mass in the "element". The derivative of the temperatures can be expressed:

$$\frac{dT}{dt} = \frac{(d/dt)U - (dC_v/dt)T}{C_v} \tag{11}$$

$(d/dt)C_v$ can be calculated directly from the equations of the mass balance for the element.

3.4. Mass transport

The mass of gas is transported throughout the dryer due to a pressure gradient. There are several ways of modeling this. A straight forward method, is to express the gas velocity out of each zone as a function of the pressure difference:

$$v_{g,i} = \frac{\sqrt{2(P_i - P_{i+1})}}{\rho_{g,i}}, \tag{12}$$

$$w_{g,i} = v_{g,i}\rho_{g,i}A_{gc} \tag{13}$$

There are two major disadvantages with this procedure. The number of state variables of the model increase as it is necessary to have the mass of dry air/gas in each volume element as a state variable. Furthermore, the model becomes stiff which influences the computation time in a negative direction. In this paper, a second approach is used based upon ideas from Moe et al. [4].

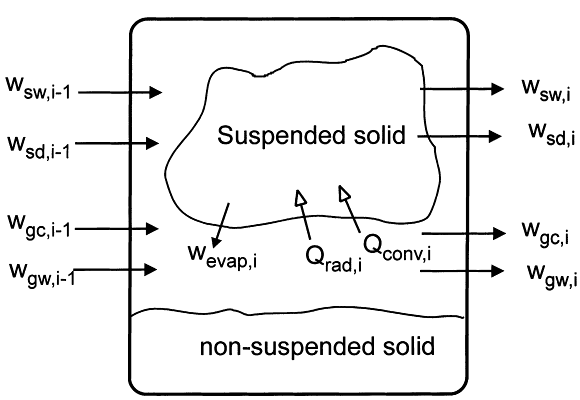

Fig. 2. Mass and heat transfer in one volume element.

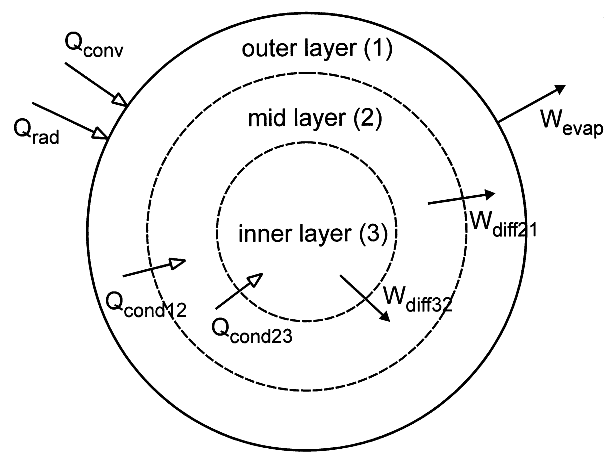

Fig. 3. Heat and mass transfer for one particle.

The balance of moles of gas in the dryer is:

$$\frac{dn}{dt} = n_{in} - n_{out} + \sum_{i=1}^{N} \frac{w_{evap,i}}{M_{H_2O}} \tag{14}$$

On the basis of the temperature gradient of the gas phase and the total number of moles of gas, the pressure in the last element is calculated. The mass transports of gas out of the last element are calculated by the Eqs. (12) and (13). In the other volume elements, the mass transport of moisture out of one zone to the next is calculated simply by addition. The molar flow out of a volume element, $j_{g,i}$, equals the molar

Table 1
State variables in a volume element

Solid phase	Gas phase
Mass of water, outer layer, $m_{sw,1}$	Mass of water (steam), m_{gw}
Mass of water, mid layer, $m_{sw,2}$	Temperature of gas phase, T_g
Mass of water, inner layer, $m_{sw,3}$	
Mass (total) of dry content, m_{sd}	
Temperature, outer layer, $T_{s,1}$	
Temperature, mid layer, $T_{s,2}$	
Temperature, inner layer, $T_{s,3}$	

flow into the volume plus the number of moles of water evaporated in the volume:

$$j_{g,i} = j_{g,i-1} + \frac{w_{evap,i}}{M_{H_2O}} \quad (15)$$

$$w_{gw,i} = j_{g,i}\frac{p_{w,i}}{P_i}M_{H_2O} \quad (16)$$

$$w_{gc,i} = j_{g,i}\frac{P_i - p_{w,i}}{P_i}M_{g,d} \quad (17)$$

The solid mass is transported along the length of the dryer by the drag force from the hot gas flow and also by mechanical transportation by the lifters. The transportation by the gas flow is considered the most important and is the only solid transport effect accounted for in the model.

According to Kelly and O'Donnel [5], the total hold up time in the dryer, T_{tot}, can be expressed empirically by the expressions:

$$T_{tot} = \frac{L_{eff}}{Y_{av}\sin\alpha + f(G)}\left(\frac{1}{2N} + \sqrt{\frac{2Y_{av}}{g}}\right) \quad (18)$$

$$Y_{av} = \frac{2D}{\pi\cos\alpha} \quad (19)$$

$$f(G) = 0.0396 v_g^{0.77} Y_{av}^{1.36} \quad (20)$$

In this case, α, the drum slope angular is zero. The expression can be reformulated and the mean velocity of the material suspended in the gas flow can be calculated by

$$v_{s,i} = \frac{f(G_i)}{\sqrt{2Y_{av}/g}} \quad (21)$$

A more rigorous approach is applied in this work. The drag force one the particles is:

$$F_D = \frac{C_D A_{part}\rho_g v_g^2}{2}\theta_D \quad (22)$$

where C_D is the drag coefficient (for a sphere):

$$C_D = \frac{1}{3}\left[\left(\frac{72}{Re}\right)^{1/2} + 1\right]^2 \quad (23)$$

The mean velocity of the suspended particles can be calculated:

$$a_s = \frac{F_D}{m}, \quad (24)$$

$$t_{fall} = \sqrt{\frac{2Y_{av}}{g}}, \quad (25)$$

$$s_{fall} = \frac{1}{2}a_s t_{fall}^2 \quad (26)$$

$$v_s = \frac{s_{fall}}{t_{fall}} \quad (27)$$

This approach gives an opportunity to account for different hold up times for different sized particles. The particles can be categorized in, e.g. three sizes. The solid phase must then be represented by the state variables, 1–7, for each size category. The different size categories will have different velocities since the volume/area ratio differs and drying rates will also differ. The model complexity increases and so does the computation time. This model will hardly be suited for an on-line control system but can be used for off-line simulations. Multiple particle sizes is not explicitly handled in this work.

3.5. Mass transfer

The driving force for the evaporation is the difference between partial pressure of water at the particle surface and the partial pressure of water in the gas;

$$w_{evap,i} = k_{evap,i}A_{s,i}(p_{ws,1,i} - p_{wg,i})\theta_k \quad (28)$$

$$p_{ws,1,i} = \exp\left(27.486 - \frac{6580}{314 + T_{s,1,i}}\right) \quad (29)$$

Mass diffusion inside the particles is expressed by

$$w_{diff,21,i} = D'_{21,i}(X_{2,i} - X_{1,i}), \quad (30)$$

$$w_{diff,32,i} = D'_{32,i}(X_{2,i} - X_{1,i}) \quad (31)$$

The diffusivity is a function of moisture and temperature:

$$D'(X,T) = D'_0\exp\left(-\frac{X_0}{X}\right)\exp\left(-\frac{T_0}{\beta + T}\right) \quad (32)$$

3.6. Heat transfer

Heat is transferred from gas to particles by radiation and convection. Heat transfer from gas to solid by convection is expressed:

$$Q_{conv,i} = h_{conv,i}A_{s,i}(T_{g,i} - T_{s,1,i})\theta_c \quad (33)$$

Heat transfer from gas to solid by radiation is calculated by

$$Q_{rad,i} = \varepsilon_i\sigma A_{s,i}(T_{g,i}^4 - T_{s,1,i}^4)\theta_r \quad (34)$$

Heat transfer by conduction from one layer to the next inside the particles can be expressed as

$$Q_{cond,12,i} = \lambda_{s,12,i}A\frac{T_{s,1,i} - T_{s,2,i}}{s}, \quad (35)$$

$$Q_{cond,23,i} = \lambda_{s,23,i}A\frac{T_{s,2,i} - T_{s,3i}}{s} \quad (36)$$

The thermal conductivity of the sugar beet is a function of temperature and water content:

$$\lambda_{s,i} = \alpha_1 + \alpha_2 T + \alpha_3 M \quad (37)$$

where M is the weight *percentage* of moisture in the beet (values for potato granular are used; $\alpha_1 = 0.0537$, $\alpha_2 = 0.00119$, $\alpha_3 = 0.00698$).

3.7. Calculation of heat and mass transfer coefficients

The heat transfer coefficient is derived from the expression:

$$Nu = 0.33\, Re^{0.6} \tag{38}$$

The expressions for Nusselts and Reynolds number are inserted and the expression for the heat transfer coefficient is obtained by

$$h_{\mathrm{conv}} = 0.33 \left(\frac{v_{\mathrm{g}} \rho_{\mathrm{g}} d_{\mathrm{part}}}{\mu_{\mathrm{g}}} \right)^{0.6} \frac{\lambda_{\mathrm{g}}}{d_{\mathrm{part}}} \tag{39}$$

The radiation emmitance coefficient ϵ is dependent on the gas temperature, the gas content of water and carbon dioxide, and on the beam length. The beam length is a function of the size and shape of the gas body surrounding each sugar beet particle. The beam length is approximately calculated as 2/3 of the diameter of the gas body volume and the gas body volume is calculated as the total gas volume of the volume element divided with the number of particles in the zone. The emmitance is calculated by a formula presented in Mehrotra [6].

The mass transfer coefficient is calculated from the link between the heat and mass transfer factors, $j_M = j_H$, where:

$$j_H = StPr^{2/3} \tag{40}$$

$$j_M = \left(\frac{k_{\mathrm{evap}}}{v_{\mathrm{g}} \rho_{\mathrm{g}}} \right) Sc^{2/3} \tag{41}$$

The values for Stantons, Prandtls and Schmidts number are inserted and an expression for the mass transfer coefficient can be obtained.

4. Model identification/verification

Plant data from a Danish sugar factory is used as a basis for the simulation studies in this paper. First, the tuning parameters are adjusted to obtain reasonable agreement between measured process variables in steady state. Plant data used in the identification are; measured dryer gas temperatures, measured gas flow, measured product moisture content, total estimated mass in dryer. The tuning parameters all have values between one and five.

It turns out that the intra-particle effects; diffusion and heat conductance, has little influence on the simulation results. A simplified model, where these effects are neglected, is used in the further simulations.

4.1. Feed variations/reference case

The major disturbances to the rotary dryer are variations in the feed of wet sugar beet slices. The feed moisture will vary due to changes in the press operation and variations in the raw material quality. The moisture of the feed is, however, unmeasured. Furthermore, the material flow inlet to the dryer is also unmeasured. There exists only a relative measurement of the feed, the conveyer belt motor speed. There is not a clear relation between feed mass flow and belt speed and this relation is not constant. This is, of course, a major problem and limitation for achieving an effective control. It is also a problem to evaluate the predictive abilities of the model, when the input to the process is not fully known.

To deal with the missing information about the feed, simulations are made with an augmented Kalman filter (AKF) versus process plant data. The AKF estimates the feed moisture content and also a measurement error in the hot gas volumetric flow. The measurements used in the estimation

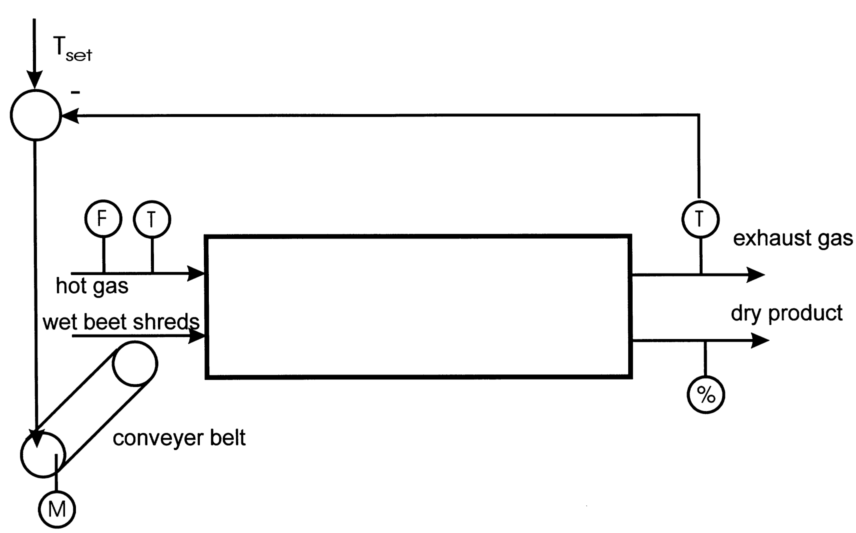

Fig. 4. Conventional feedback control of rotary dryer.

are; inlet gas flow, temperature of inlet gas and conveyer belt speed as inlet variables and product moisture and outlet gas temperature as outlet variables. A data set of 500 samples with a sampling interval of 5 min is used. The AKF is applied to the model and plant data several times. The simulation with the AKF is run with the estimated disturbances from the previous simulation as additional input data. The final estimates of the product moisture are shown in Fig. 4. When these values are applied to the model, there is a quite good agreement between measured and predicted values.

5. Process control

The most important control loop for the rotary dryer is the control of product moisture. The coal-fired burner is not suitable as a manipulated variable, one of the reasons being its rather slow dynamics. Instead, the feed of sugar beet pulp is used as a manipulated variable to control the product moisture in a feedback control loop as shown in Fig. 5. The measured product quality is not used directly in the control loop. There is a large time delay for the effect of a change in the feed to a change in product moisture. The product moisture is correlated to the gas exhaust temperature, which is used as an indicator for the product moisture and used in the product quality feedback loop.

5.1. Control simulations

The traditional feedback control configuration is simulated with the reference case, i.e. the disturbances estimated by the AKF and the measured hot gas temperatures. The control loop does counteract for the disturbances to some extent. The gas exhaust temperature is held within rather narrow limits (Fig. 6). The gas temperature is, however, a rather poor indicator for the product moisture, which shows large variations (Fig. 7).

The same case is simulated with a model based predictive controller (MPC) configuration. The controller is a standard dynamic matrix control (DMC) algorithm. An important feature in this case is, however, that the DMC system matrix, containing information about the dynamic behavior of the process, is obtained by perturbation of the non-linear state variable model in each control time sample. The control sample interval is chosen to be 30 s. It is assumed that the disturbances are measurable. The controller gives excellent control of the product moisture (Fig. 8). The gas exhaust temperature is allowed to vary (Fig. 9).

In the last simulation it is assumed that the disturbances are not measurable, which is the case at the

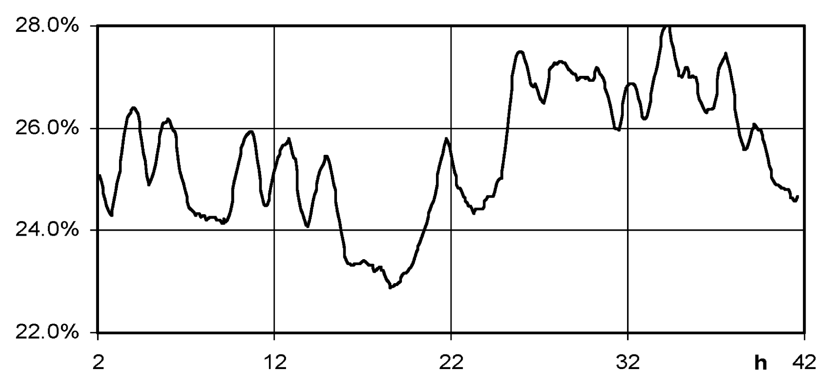

Fig. 5. Estimated feed moisture (by the AKF).

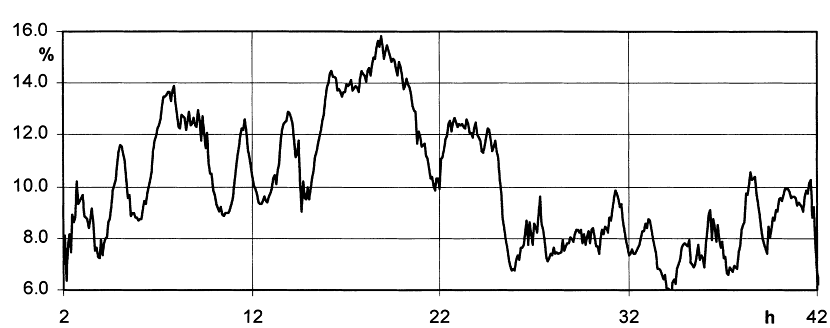

Fig. 6. Exhaust gas temperature, conventional control.

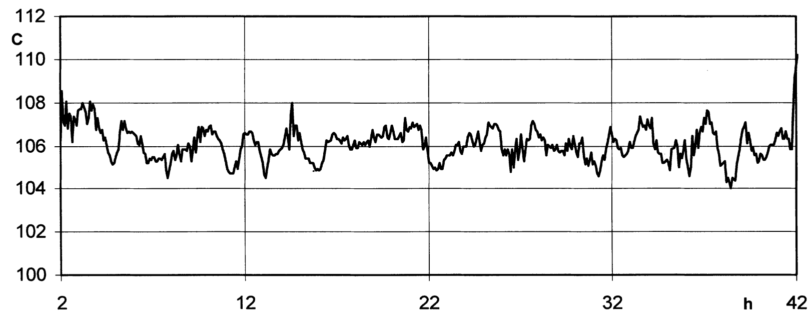

Fig. 7. Product moisture, conventional control.

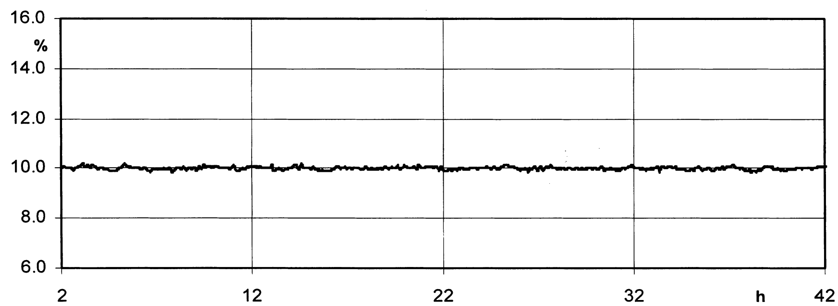

Fig. 8. Product moisture, MPC.

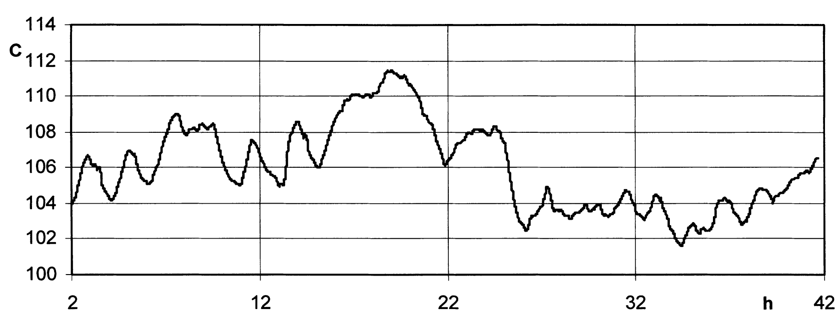

Fig. 9. Exhaust gas temperature, MPC.

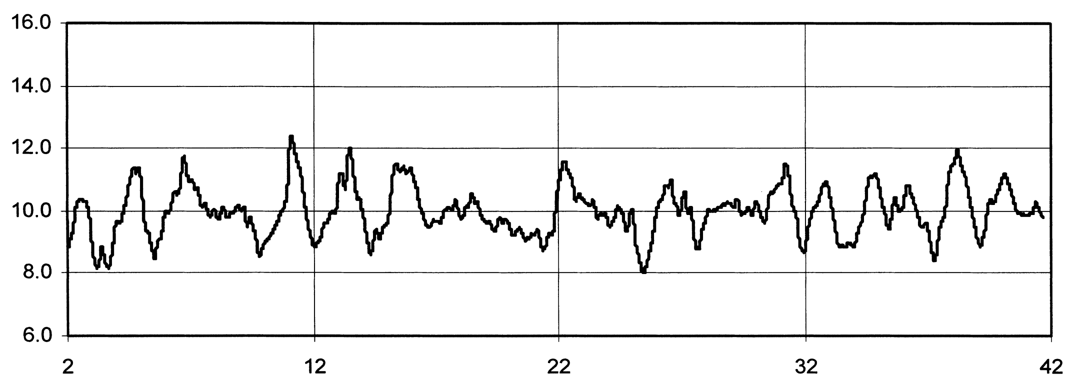

Fig. 10. Product moisture, MPC and AKF.

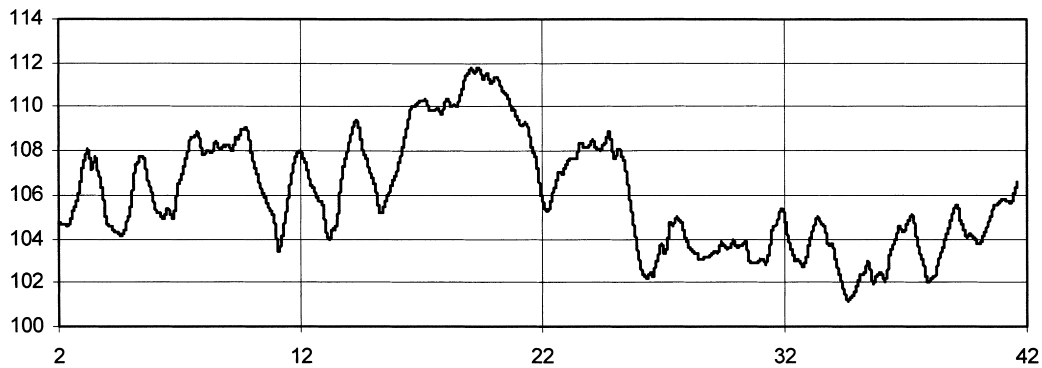

Fig. 11. Exhaust gas temperature, MPC and AKF.

specific factory. The disturbances are instead estimated by the AKF and the estimated disturbances are used in the MPC. The performance is not quite as good as in the case of measured disturbances but on the other hand clearly better then the traditional feedback approach (Figs. 9–11).

6. Conclusion

A dynamic model of a rotary drum dryer has been developed. The model is shown to have good predictive capabilities. The model is used in a MPC. The MPC is compared with traditional feedback control in a simulation study based upon industrial plant data. The performance of the MPC is superior. In the case of unmeasured input disturbances, an AKF is used to estimate the disturbances. This approach gives a fairly good result.

Acknowledgements

This work is partly financed by the Danish energy agency.

References

[1] D. Marinos-Kouris, Z.B. Maroulis, Transport properties in the drying of solids, in: A.S. Mujamdar (Ed.), Handbook of Industrial Drying, 2nd Edition, Dekker, New York, 1995, pp. 113–159.
[2] F. Courtois, Dynamic Modelling of Drying to Improve Processing Quality of Corn, Ph.D. Thesis report, ENSIA, Massy, France, 1991.
[3] H.R. Perry, D.W. Green, Perry's Chemical Engineers' Handbook, 7th Edition, McGraw-Hill, New York, 1997.
[4] H.I. Moe, H.C. Riksheim, T. Hertzberg, Stiffness reduction of gas system models, Comput. Chem. Eng. 20 (Suppl.) (1996) 901–906.
[5] J.J. Kelly, J.P. O'Donnel, Dynamics of granular material in rotary dryers and coolers, IChemE Symp. Series no. 29, 1969.
[6] A.K. Mehrotra, K. Karan, L.A. Behie, Estimate Gas Emissivities for Equipment and Process Design, Chemical Engineering Progress, 1995, pp. 70–77.